Supplementary Appendix

This appendix has been provided by the authors to give readers additional information about their work.

Supplement to: Stoner R, Chow ML, Boyle MP, et al. Patches of disorganization in the neocortex of children with autism. N Engl J Med 2014;370:1209-19. DOI: 10.1056/NEJMoa1307491

Appendix

1. Detailed Methodology

1.1 Tissue preparation

To examine cortical microstructure, we performed histological and laminar-specific marker ISH analyses on DL-PFC tissue blocks from a large sample of young autistic and control male and female subjects, and on temporal and occipital blocks from a small sample of young autistic and control male subjects.

1.1.1 Cases

A total of 42 frozen postmortem cortical tissue blocks (1-2 cm^3) from the superior or middle frontal gyrus, the posterior superior temporal cortex (pSTC) and occipital cortex (BA17) were obtained from the National Institute of Child Health and Human Development, University of Maryland (NICHD/UMB) Brain and Tissue Bank and from the Autism Tissue Program (ATP). All autism cases met criteria for autistic disorder on the Autism Diagnostic Interview-Revised[1] (ADI-R), the Autism Diagnostic Observation Schedule[2] (ADOS), or were diagnosed by medical records. The ADI-R was administered postmortem by brain and tissue banks using standard procedures. In one autistic child, the ADOS had been administered pre-mortem. All of the obtained tissue samples were tested for quality and the blocks with the highest quality were chosen for sectioning, histology, and ISH. Thirty-one frozen blocks from 11 autism and 11 control male and female cases 2-15 years of age passed quality control for histological and ISH analysis (Table S2).

Cases were not selected for any reason, such as autopsy brain weight, postmortem interval (PMI), cause of death or specific clinical characteristics (other than an ASD diagnosis), except that the prefrontal, temporal and occipital cortical tissue met the tissue quality control requirements stated below.

Perinatal and postnatal medical conditions were obtained by the tissue banks from next-of-kin. Cause of death, PMI, and neuropathology were obtained from coroner's reports. Race of each postmortem case was determined by the tissue banks from information gathered from next-of-kin, and race and ethnicity categories were based on National Institutes of Health requirements. Research procedures were approved by the institutional review board of the University of California, San Diego. Informed consent or waiver of consent was not required because all cases were deceased, de-identified and anonymized by the tissue banks.

All autism diagnostic classifications were based on the results of postmortem administration of the Autism Diagnostic Interview-Revised (ADI-R) to a parent or legal guardian of the deceased by a psychologist, which is the standard method for autism postmortem research. The ADI-R is a standardized parent interview used for determining developmental history and behavior for the purposes of diagnosing autism. Questions are designed to elicit relevant information through queries closely associated with diagnostic criteria set forth in the Diagnostic and Statistical Manual of Mental Disorders-IV. The administration, scoring and diagnostic determination is the same as when it is administered to the parent or legal guardian of a living individual. Determination of the intellectual ability level of each autistic child was done blind to knowledge of the neuropathology and neuron counts. Non-intellectual disability was defined as IQ of 71 or above on standardized IQ tests or evidence from the ADI-R Narrative of understanding of most words and sentences, communicative use of words and language, and some initiation of appropriate activities such as looking at books, using computers, showing some interest in mother or playing games. Intellectual disability was defined as IQ equal to 70 or below or little to no understanding or use of words and lack of appropriate activities, presence of self-injurious behavior and/or non-responsiveness to others.

All control cases came from the NICHD Brain and Tissue Bank. This tissue bank determined control cases to be free of mental illness, intellectual disability, and neurological disorder, including autism, based on information gathered in a detailed questionnaire at the time of death from next-of-kin. Cases with a history of chemotherapy/radiation treatment or being resuscitated following ischemic hypoxia are excluded as controls by the tissue banks.

1.1.2 Sample collection

Due to documented variability of even neighboring brain areas[3,4], it was important that the blocks of tissue were from comparable regions between cases. Every available control and autistic case under the age of 16 with frozen tissue in these locations was requested from these resources for these experiments. Working directly with the neuroanatomy experts at each brain bank, anatomical landmarks were identified as consistently as possible for dissection across cases with the goal of obtaining a set of highly controlled, comparable tissue for brain gene expression profiling. When available, tissue from the superior frontal gyrus of the dorsal lateral prefrontal cortex (DL-PFC; Brodmann's Area 9/46) was dissected in each case. When this area was not available, we sampled from the middle frontal gyrus of DL-PFC. pSTC samples were dissected from BA22, and occipital samples were taken from BA17.

1.1.3 Tissue quality control

Prior to processing, all tissue samples were tested for (a) RNA quality, (b) absence of severe ice crystal artifacts, and (c) suitability for tissue morphology analyses. For RNA quality assessment, two tissue sections weighing between 2-5mg were collected. RNA was extracted using the MELT™ Total Nucleic Acid Isolation system (Ambion, Foster City, CA), per manufacturer's protocol. RNA quality was determined for each specimen using high-resolution capillary electrophoresis on an Agilent Bioanalyzer 2100 (Agilent Technologies, Palo Alto, California) and Agilent's RNA Integrity Numbers (RIN) software algorithm to generate RINs (Schroeder et al., 2006). RNA was eluted in 20 µl nuclease-free water, standardized to a concentration of 5 ng/µl, and 1 µl was run on a Pico Bioanalyzer chip. Tissue samples with a RIN value below 5 were excluded from further study.

Tissue quality was further assessed by taking a representative section from each sample and staining with a regressive Hematoxylin and Eosin (H&E) stain**.** Slides were fixed for 20 minutes in 4% neutral buffered paraformaldehyde (PFA) and rinsed in 1x PBS, acetylated for 10 minutes in 0.1M triethanolamine with 0.25% acetic anhydride, dehydrated using a graded series of 50%, 70%, 95% and 100% ethanol, and stained first with commercially prepared Harris hematoxylin for 20 min, differentiated in 1% HCl in 70% ethanol for 15-30 sec, blued with 1% lithium carbonate for 1 min and stained in 1% eosin Y in 1% aqueous calcium chloride for 3 min. Sections were then dehydrated in a graded series of 70%, 95% and 100% ethanol, cleared in xylene and coverslipped with either DPX or CureMount mounting media.

The presence of distributed large ice crystals was grounds for excluding cases from ISH processing. All cases used passed the RIN analysis; however, due to the scarcity of high quality tissue, some samples with less than optimal tissue morphology were included in the study. Autism case B6399 had mild ice crystal damage but was included because this case was younger than any postmortem case that had been examined to date and preliminary results indicated that it was possible to obtain robust ISH signal on the tissue.

Two additional cases (8 and 21) showed mild to moderate tissue damage but were included because they each contained some regions of preserved morphology and the physical damage was less severe than other available cases. Following quality control, tissue samples from the DL-PFC, pSTC, and occipital cortex of 11 autistic male and female postmortem cases ages 2 to 15 years old and

from 11 control postmortem cases 4 to 15 years old were selected for the current experiments. Detailed clinical information is provided in Table S2.

1.1.4 Sectioning procedure

Leica CM2050 S cryostats were used to section the frozen tissue samples at 20 µm thickness in a plane that would best equally show 6 layers of cortex and white matter. Sections were serially placed on slides in 5 sets of 30. Slides were organized into groups of 5, representing 10 tissue sections spaced 600 µm apart. Sets 15 and 30 were stained with Nissl for cytoarchitectural and anatomical reference, so that these sections occurred every 300 µm throughout the tissue block.

Briefly, slides were cleared with Xylene or Formula 83 for 30 minutes, rehydrated using a graded series of 100%, 95%, 70% and 50% ethanol, rinsed with water, stained with 0.21% Thionin for 1 minute, rinsed with water, dehydrated using a graded series of 50%, 70%, 95% and 100% ethanol, cleared with Formula 83 or Xylene, and coverslipped. Following sectioning, the remaining slides were allowed to air dry and tissue was fixed, acetylated and dehydrated. Tissue was fixed for 20 minutes in 4% neutral buffered paraformaldehyde (PFA), rinsed in 1x PBS, acetylated for 10 minutes in 0.1M triethanolamine with 0.25% acetic anhydride, and dehydrated using a graded series of 50%, 70%, 95% and 100% ethanol. Slides were stored at -80°C in vacuum-sealed slide boxes until used.

1.2 In Situ Hybridization Procedure

1.2.1 Gene selection

In order to select the genes for the experimental study, a preliminary screen was performed to assess the feasibility of performing ISH on adolescent human brain tissue and to identify genes with robust expression patterns in the DL-PFC that were consistent across ages. Sixty-three genes (Table S1) were analyzed including ones likely to show lamina- and cell type-specific expression patterns and genes implicated in the pathogenesis of autism. Their expression patterns were analyzed in DL-PFC postmortem tissue samples from 2 control males (10 and 16 year old males) in order to identify markers with robust, consistent, and specific expression patterns. Twenty-four laminar-specific genes were selected for Study I, comparing gene expression of young male autism and control cases.

Study II aimed to investigate whether the prefrontal patches we discovered in autistic males in DL-PFC also occur in autistic females and in temporal cortex (a region implicated by MRI, and fMRI studies of living patients) but not in occipital cortex (a region that is commonly not abnormal on fMRI and MRI studies). We reasoned that a strong test of the patch discovery in Study I would be to select the four excitatory neuron subtype-selective ISH markers that were most frequently abnormal in Study I, namely *CALB1*, *RORB*, *PCP4* and *PDE1A*, to see if in a new set of cases they would again be abnormal in patches and indeed they were.

We selected *NEFL* because it is a ubiquitous neuron marker and would tell us qualitatively whether reduced expression of *CALB1, RORB, PCP4 and PDE1A* in patches was associated with reduced numbers of neurons. Thus, while Study I used Nissl sections to tell us whether neuron numbers are reduced in patches, in Study II *NEFL* enabled us to compare “like to like” (ISH layer-specific markers to ISH neuron markers) to see if neurons in general are reduced where ISH layer markers are reduced.

1.2.2 ISH probe design and synthesis

RefSeq sequences were input into a Primer3 software-based semi-automated process (Whitehead Institute for Biomedical Research) to design probes. Probes were between 400-1000 bases long and contained less than 200 bp with greater than 90% homology to non-target transcripts. Standard *in vitro*

transcription reactions based on PCR templates from human cDNA clones or pooled cDNA synthesized from human brain total RNA were used to generate riboprobes.

Roche's 10X DIG RNA Labeling Mix was used in 30 μL volume reactions in 96-well formats for standard IVT reactions for 2 hours at 37°C. SP6 RNA polymerase (NEB) was used on the purified PCR product templates, and IVT reactions were purified using the Millipore Montage 96 filter plate. Subsequent to a 30-minute room temperature incubation, reactions were eluted with 90 μL of THE (Ambion). The RiboGreen HIGH Assay (Molecular Probes), Agilent's Bioanalyzer 2100, and the SpectraMax-M2 plate reader were utilized to quantify IVT reactions and to confirm size. Following stringent quality control measures and dilution, IVT reactions were then stored at -80°C. Details of this reaction are outlined in the Allen Institute's technical white paper (http://help.brain-map.org/download/attachments/2818165/HBA_ISH_WhitePaper.pdf?version=1&modificationDate=1361836502217).

1.2.3 Colorimetric ISH

A colorimetric, digoxigenin-based method for labeling target mRNA was used to detect gene expression[4]. In brief, slides were placed on temperature-controlled racks of flow-through chambers on computer controlled Tecan Genesis liquid handling platforms. The tissue was then permeabilized, endogenous peroxidase activity blocked, and digoxigenin-labeled probes were hybridized to target mRNA followed by washing to remove excess probe. Slides were then incubated with a horseradish peroxidase (HRP)-conjugated anti-digoxigenin antibody and a biotin-coupled tyramide. Biotin was bound to alkaline phosphatase-conjugated neutravidin and BCIP/NBT, which formed a blue/purple precipitate. Finally, washing with EDTA and fixation with 4% PFA stopped the reaction. After the completion of the run, the slides were counterstained with Feulgen-HP Yellow. Slides were washed with an acid alcohol (70%, adjusted to pH = 2.1 with 12 N HCl) rinsed with milliQ water, incubated in 5N HCl, rinsed, stained with HP Yellow (Anatech Ltd) for 20 minutes, rinsed, washed with acid alcohol, and rinsed again before coverslipping. High-resolution images were acquired using ScanScope® scanners (Aperio Technologies, Inc; Vista CA). Additional protocol details can be found at http://help.brain-map.org/download/attachments/2818165/HBA_ISH_WhitePaper.pdf?version=1&modificationDate=1361836502217.

1.3 ISH Image Examination and Visualization

1.3.1 Expert anatomist-based ISH analysis

Since staining patterns of each gene were consistent throughout control cases, deviations in gene expression observed in autism cases could confidently be assessed as abnormal. An ISH abnormality index was developed to characterize the relative degree of abnormality for each gene in every autism case when compared to control ISH. Two investigators independently (one at UCSD and one at the Allen Institute) analyzed the ISH data in each case and scored all genes on a three-point scale, 0 for normal, 1 for subtle abnormality, and 2 for significant abnormality. Abnormality was based on the criteria that across more than 3 sections and compared with controls: i) laminar gene expression appeared disrupted; ii) gene expression within layers or across layers appeared deficient by a qualitative change in the number or intensity of labeled cells compared with adjacent areas; iii) the laminar gene expression pattern appeared disrupted compared with adjacent areas; and iv) cell type- or lamina-specific gene expression appeared misplaced. Correlation between the two independent raters was 86% of 181 observations. Assessments that differed between the two expert anatomists were identified and reassessed to form a collaborative judgment. Results are presented in Table 2 of the main text. Full resolution raw image data is available online through the Allen Brain Atlas data portal (http://www.brain-map.org) or at (http://human.brain-map.org/ish). Selected raw image data has been included in supplemental Figures S1-S4 along with overlays of autism case 12 and case 15 (Figure S5).

1.3.2 Three-dimensional reconstruction of laminar structure

To generate three-dimensional reconstructions of laminar microstructure, an image-processing pipeline was developed (Figure S6). The pipeline is comprised of three parts: A, stack registration; B, expression point cloud extraction; C, two-dimensional convolution to generate a pseudo-density volume.

1. To perform the image registration, tissue regions were segmented from raw images, cropped, and downsampled to 2,000 pixels by 1,500 pixels for an effective resolution of 1 pixel/16μm using ImageJ. The downsampled image was then filtered using a filter chain that produced an ISH-marker invariant version. Images were then registered serially using ITK with a centered rigid body transformation. Transforms generated by the registration process were stored in plaintext files for later steps.
2. To perform point cloud extraction, tissue regions were segmented from raw images and cropped. The cropped image, still at a native resolution of 1pixel/1μm, was filtered using a fixed RGB threshold to remove the background signal from the ISH label. A particle analysis was performed using ImageJ to extract objects within a certain size threshold (>4μm, <64μm). The point cloud data for each image was stored to a plaintext file for later steps.
3. To reconstruct the pseudo-expression volume of the laminar microstructure, point cloud data from each image was transformed by a scaled version of the centered 2D transform calculated from the initial stack registration. Pseudo-expression maps were produced by applying a 2D Gaussian convolution to the transformed point cloud data. Each map was merged into a stack of 10 serial images. A linear interpolation was then applied between frames to estimate the expression density between each key frame. Volumes for several ISH markers were then rendered within a single visualization environment (UCSF Chimera) to produce the three-dimensional reconstruction of the laminar microstructure and patch regions.

The reconstruction workflow was built using open source tool-chains (ITK, ImageJ) and organized using python and C++ programming languages. Source code for the workflow is available upon request. Stepwise reconstruction of a control cases is presented in Figure S7.

1.4 Blinded Stereological Analyses of Neuron and Microglial Density and Volume

Blinded and unbiased stereological analyses of neuron and microglia number and volume were performed by an independent research team at the Stereology Resource Center (SRC; P.M., M.B., J.B.) Analyses were blinded to the purpose of the study, research design, and our ISH findings. Slides submitted for stereology were coded once by UCSD, and again by the SRC. To ensure that microglia were not incorrectly counted as neurons, neurons and microglia were identified, counted and measured separately. Analyses examined neuron and microglia cell size distributions.

1.4.1 Definition of regions of interest for stereological quantification

Blinded stereological quantification was carried out in the DL-PFC of all 16 young male cases (N=8 autism and N=8 control) based upon the regions marked by the neuropathologist (S.R.). Due to the fact that gender differences in neuron densities in human cortex have been shown in a number of studies and our sample included only 3 females per study group, stereology and statistical analyses were performed on male cases only. Pan-laminar density quantification measurements were made in patch and one non-patch region in each ASD case, and two representative regions in control cases, utilizing a computerized stereology system (*Stereologer*, Stereology Resource Center, Chester, MD).

Our original intention was to investigate the differences in density within individual lamina of both the patch and non-patch areas. However, due to the cortical disorganization observed in the autistic cases, definition of lamina was not reliable. Additionally, though it was possible to use laminar marker information to delineate the layers of the cortex in control individuals, the decrease in expression of these markers in patch regions rendered this approach unreliable in autistic cases. Thus, we chose to carry out the stereological analysis across pan-laminar regions.

For each case, the two regions in each section were separately outlined at lower power (5x) and neuronal counts for each region quantified using high magnification (63x, 1.4 n.a. oil-immersion). Pan-laminar regions included an equal representation of each lamina and were traced in a columnar fashion to include all six layers of cortex, avoiding artifacts. The pial surface and the grey-white boundary were defined using cortical cytoarchitecture, along with cellular structure and appearance[5,6]. Quantification for each region in each case was done on a minimum of 5 sections stained with Nissl using an inter-slide interval of approximately 600 microns, *i.e.*, every other Nissl section.

1.4.2 Blinded stereological quantification of neuron and microglia density and size

Density of neurons and microglia in two pan-laminar reference spaces per case were quantified on Nissl-stained sections using the optical fractionator method, which is a combination of the disector principle, fractionator sampling scheme, and unbiased counting rules as previously detailed[7-10]. A guard volume was used to avoid uneven section surfaces, lost caps and other sectioning artifacts. A total of 100-150 neurons per reference space were sampled to achieve a high level of sampling stringency, *i.e.*, mean coefficient of error (CE) 0.10 or less[7]. Criteria for counting cells required that they have the morphological features consistent with neurons and glia. The mean cell volume (MCV) was estimated using the rotator principle[11] as previously described[12].

Analysis of variance with a threshold of $p<0.05$ was used to compare estimates of average neuron and microglia density and mean cell volume in control cases to that of the patch and non-patch areas in autistic cases. Combined group averages were also compared using two-tailed student t-tests.

The one-factor ANOVA revealed no significant differences in neuron volume, neuron density, glia volume, or glia density between groups across the independent stereological regions (N=8 per region). When grouped by diagnostic category, a small but significant increase in neuron density in the autism cortex (two-tailed T, p=0.031, N=16 per group) relative to control cortex was identified (Figure S8).

It is important to note that this analysis was limited in scope due to the small amount of sample analyzed and lack of sufficient sampling to estimate tissue-level measurements.

1.5 Post-hoc qPCR quantification of patch region

1.5.1 Experimental approach and discussion of results

A second approach was used to further characterize and validate the colorimetric ISH results, namely, laser microdissection (LMD) in combination with quantitative RT-PCR within a patch of reduced ISH expression relative to immediately adjacent cortex. Ideally, this would have been performed using LMD on frozen sections from Studies I and II. Unfortunately, insufficient tissue remained from the original samples to perform such an experiment.

To overcome this limitation, a new experiment was performed using additional tissue blocks of DL-PFC from four autistic cases that had robust evidence of patches from the Studies I and II. Each block was processed as described in sections 1.1-1.3 with two changes: 1) a reduced panel of laminar and cell-type specific markers was used and 2) half of all sections from each series were set aside for LMD and qPCR quantification.

Patch-like regions were identified using the criteria established in Section 1.3.1 in two of the four blocks examined. The most prominent patch was found in tissue from Case 20 and selected for LMD and qPCR quantification using methods outlined below (Section 1.5.2). Results from the qPCR experiments displayed a greater-than 11-fold decrease in *CALB1* expression when compared to adjacent cortex (Figure 3).

This result strongly supported the premise that the identified decreases in numbers of *CALB1* labeled cells in the ISH images corresponds to a decrease in expression of the respective marker. Further interpretation of qPCR results from this experiment is limited at this time due to the lack of sufficient amount of material for extensive qPCR from this region.

1.5.2 Laser microdissection and RT-qPCR methodology

After tissue was validated, 20 µm tissue sections were collected onto PEN (polyethylene napththalate) membrane slides for LMD or standard glass slides for ISH and thionin-based Nissl staining, respectively. LMD was performed using a Leica LMD6000 system on regions of interest (ROI) that were defined by ISH on interleaved tissue sections. Two Sensiscript cDNA reactions per ROI were done, each reaction using 40ng total RNA as input. cDNA was then pooled across the same ROI. Real-time qPCR was conducted using *CALB1* gene-specific primer pairs, including *GAPDH* positive control primer pairs, using Roche Lightcycler 480 SYBR Green on the Roche LightCycler 480 System. Difference in number of cycles needed to reach a threshold level of fluorescence with gene-specific primers as compared with GAPDH primers (ΔCp) was used as a measure of relative mRNA abundance.

2. Supplemental Tables

2.1 Table S1 – 63 Candidate genes used for ISH pilot

Sixty-three candidate lamina-specific, cell-type specific or autism-relevant markers tested on two control samples in the pilot phase, and the rationale for gene selection. Images of this dataset are available on request. 25 genes were chosen from this set for the final experiment, of which 24 were used in Study I and 5 in Study II.

2.2 Table S2 – Male and female complete subject details

Available clinical information is provided for autistic and control cases in this study. Assessments were made by a clinical psychologist (C.C.B.). HX = History; DO = Diagnosis; IVF = In Vitro Fertilization; PMI = Postmortem Interval.

2.3 Table S3 – Male and female subject diagnosis details

Available clinical information, including information from the ADI-R assessment, noted seizure activity and intellectual disability, is provided for autistic cases in this study. Assessments were made by a clinical psychologist (C.C.B.). ADI = Autism Diagnostic Interview; RIN = RNA Integrity Score; HX = History; DO = Diagnosis; ADI Comm Score = ADI-R Communication Score; ADI R&R Score = ADI-R Restricted and Repetitive Behavior Score; IVF = In Vitro Fertilization.

<Tables S1-S3 on following three pages>

Gene Symbol	Gene Name	Entrez Gene ID	Marker	Study I	Study II
AIF1	Allograft inflammatory factor 1	199	Microglia	x	
B3GALT2	UDP-Gal:betaGlcNAc beta 1,3-galactosyltransferase, polypeptide 2	8707	Layer 6		
NDNF	neuron-derived neurotropic factor	79625	Layer 1	x	
CALB1	Calbindin 1, 28kDa	793	Layer 2/3	x	x
CALB2	Calbindin 2, 29kDa (calretinin)	794	Interneurons	x	
CART	Cocaine- and amphetamine-regulated transcript	9607	Layer 3b		
CDH24	Cadherin-like 24	64403	Layer 6		
CNR1	Cannabinoid receptor 1 (brain)	1268	Layer 2/3		
CNTNAP2	Contactin associated protein-like 2	26047	Autism candidate	x	
COL24A1	Collagen, type XXIV, alpha 1	255631	Layer 5/6		
CPNE7	Copine VII	27132	Interneurons		
CRH	Corticotropin releasing hormone	1392	Interneurons		
CSRP1	Cysteine and glycine-rich protein 1	1465	Oligodendrocytes		
CTGF	Connective tissue growth factor	1490	Layer 6b	x	x
CTNND2	Catenin (cadherin-associated protein), delta 2 (neural plakophilin-related arm-repeat protein)	1501	Autism candidate		
CUTL2	Cut-like 2 (Drosophila)	23316	Layers 2-4		
CXCL14	Chemokine (C-X-C motif) ligand 14	9547	Interneurons	x	
DISC1	Disrupted in schizophrenia 1	27185	Layer 1		
ETV1	Ets variant gene 1	2115	Layer 5		
FOXP2	Forkhead box P2	93986	Layer 6	x	
GABRB3	Gamma-aminobutyric acid (GABA) A receptor, beta 3	2562	Autism candidate		
GABRG1	Gamma-aminobutyric acid (GABA) A receptor, gamma 1	2565	Layer 4		
GAD1	Glutamate decarboxylase 1 (brain, 67kDa)	2571	Interneurons	x	
GAD2	Glutamate decarboxylase 2 (pancreatic islets and brain, 65kDa)	2572	Interneurons		
GFAP	Glialfibrillary acidic protein	2670	Astrocytes		
HTR1A	5-hydroxytryptamine (serotonin) receptor 1A	3350	Layer 2/3		
KIT	v-kit Hardy-Zuckerman 4 feline sarcoma viral oncogene homolog	3815	Interneurons		
LGALS1	Lectin, galactoside-binding, soluble, 1 (galectin 1)	3956	Layer 5/6		
LGI2	Leucine-rich repeat LGI family, member 2	55203	Interneurons		
MBP	Myelin basic protein	4155	Oligodendrocytes		
MFGE8	Milk fat globule-EGF factor 8 protein	4240	Layer 3	x	
MYBPC1	Myosin binding protein C, slow type	4604	Layer 5/6	x	
NEFL	Neurofilament, light polypeptide	4747	Neurons		x
NLGN3	Neuroligin 3	54413	Autism candidate		
NLGN4X	Neuroligin 4, X-linked	57502	Autism candidate		
NPY	Neuropeptide Y	4852	Interneurons		
NPY2R	Neuropeptide Y receptor Y2	4887	Interneurons		
NRXN1	Neurexin 1	9378	Autism candidate	x	
NTNG2	Netrin G2	84628	Layer 5/6	x	
PCP4	Purkinje cell protein 4	5121	Layer 5/6	x	
PDE1A	Phosphodiesterase 1A, calmodulin-dependent	5136	Layer 5/6	x	x
PDYN	Prodynorphin	5173	Interneurons		
PENK	Proenkephalin	5179	Layer 2/3		
PPAP2B	Phosphatidic acid phosphatase type 2B	8613	Astrocytes		
PRKCB1	Protein kinase C, beta 1	5579	Autism candidate	x	
PVALB	Parvalbumin	5816	Interneurons	x	
PVRL3	Poliovirus receptor-related 3	25945	Layer 2/3		
RELN	Reelin	5649	Layer 1	x	
RORB	RAR-related orphan receptor B	6096	Layer 4	x	x
SCN4B	Sodium channel, voltage-gated, type IV, beta	6330	Layer 4		
SLC1A2	Solute carrier family 1 (glial high affinity glutamate transporter), member 2	6506	Astrocytes	x	
SLC6A1	Solute carrier family 6 (neurotransmitter transporter, GABA), member 1	6529	Interneurons		
SST	Somatostatin	6750	Interneurons	x	
SV2C	Synaptic vesicle glycoprotein 2C	22987	Layer 5		
SYNPR	Synaptoporin	132204	Interneurons	x	
SYT6	Synaptotagmin VI	148281	Layer 5		
TAC1	Tachykinin, precursor 1	6863	Interneurons		
TAC3	Tachykinin 3 (neuromedin K, neurokinin beta)	6866	Interneurons		
TLE4	Transducin-like enhancer of split 4 (E(sp1) homolog, Drosophila)	7091	Layer 6		
TOX	Thymus high mobility group box protein TOX	9760	Layer 5		
VAMP1	Vesicle-associated membrane protein 1 (synaptobrevin 1)	6843	Layer 4/5		
VAT1L	vesicle amine transport protein 1 homolog (T. californica)-like	57687	Layer 5	x	
VIP	Vasoactive intestinal peptide	7432	Interneurons	x	

Case	1	2	3	4	5	6	7	8	9	10	11
Age	4	4	4	7	8	9	10	12	12	14	15
Gender	F	M	M	M	M	F	M	M	M	M	F
Diagnosis	Control	Control	Control	Control	Control	Control	Control	Control	Control	Control	Control
Race	Asian	Caucasian	Caucasian	Caucasian	Caucasian	African American	Caucasian	African American	African American	Caucasian	Caucasian
Hx Meds	Tylenol to control fever	Atropine and Epi at death scene to revive heart with no response	None reported	Concerta and Clonodine	None reported	Albuterol, Zyrtec, Allegra, Flovent, Flonase	None reported	None reported	Singulair, Albuterol, Prednisone, Claritin	None reported	None reported
Prenatal Hx	None reported	None reported	None reported	None reported	None reported	None reported	None reported	None reported	None reported	None reported	None reported
IVF/ Fertility Hx	None reported	None reported	None reported	None reported	None reported	None reported	None reported	None reported	None reported	None reported	None reported
Psych DO in Family	None reported	None reported	None reported	None reported	None reported	None reported	None reported	None reported	None reported	None reported	None reported
Cause of Death	Lymphocytic Myocarditis	Drowning	Commotio Cordis	Drowning	Cardiac Arrhythmia	Asthma	Sudden Unexplained Death in Childhood (SUDC)	Cardiac Arrthymia	Asthma	Multiple injuries	Chest Injuries
PMI	21	17	17	12	5	20	24	22	15	16	5
RIN	6.8	2.2	7.6	7.7	7.5	7.6	7.3	7.7	6.5	7.7	8.8
Comments	child was adopted and lived in orphanage where she was reported to have pneumonias; had a recent history of flu and fever	drowned at beach; HIV negative	cardiac arrest immediate following baseball to sternum; HIV negative	Diagnosed with hyperactive disorder; premature gestation of 5-6 months	Child had cardiac issues, diagnosed with abnormal coronary artery several days before he died; autopsy results indicated inflammatory myofibroblastic tumor of the aortic valve; HIV negative	collapsed, died in transit to hospital, HIV negative	Diagnosed with polymyosis (uncommon connective tissue disease with inflammation) and undergoing evaluation at time of death; HIV negative	history of high cholesterol and enlarged heart; HIV negative	HIV negative, history of asthma and peanut & apple allergies	ATV accident; non smoker; HIV negative	passenger in car accident; HIV negative

Case	12	13	14	15	16	17	18	19	20	21	22
Age	2	4	5	5	7	8	8	8	9	14	15
Gender	M	F	F	M	M	M	M	M	M	M	F
Diagnosis	Autism	Autism	Autism	Autism	Autism	Autism	Autism	Autism	Autism	Autism	Autism
Race	Japanese, Native American, Caucasian, Hispanic	African-American	Asian	Caucasian	African-American		African American	African-American	Caucasian	Caucasian	Caucasian
Hx Meds	None reported	None reported	None reported	Repeated antibiotics due to ear infections	Inpatient chelation due to lead poisoning (plumbism) @ age 3	Depakote, Chemotherapy	Zyprexa, Reminyl, Adderal	None	Desipramine (antidepressant) for ADD	Trileptal, Zoloft, Clonidine, Melatonin	Depakote, Prozac, Kepra; Carbamazapine, Phenyltoin, Klonopin, Lamotrigine, Felbamate, Valproic acid
Prenatal Hx	Repeated C-Sec, mother miscarried twice; slight jaundice at birth, slightly blue at birth, got oxygen	Nothing remarkable reported	Adopted; not known	Fallen cervix during pregnancy; occasional cigarette use during pregnancy; no alcohol use; induced labor	Full term, cesarean; heroine, cocaine, alcohol and cigarette use during pregnancy; child hospitalized with withdrawal for first 3 weeks of life	Nothing remarkable reported	Nothing remarkable reported	Nothing remarkable reported	Nothing remarkable reported	Nothing remarkable reported	Nothing remarkable reported
IVF/ Fertility Hx	None reported	None Reported	Adopted; not known	None reported	None reported	None reported	None reported	None reported	None reported	None reported	None reported
Psych DO in Family	Maternal 3rd cousin with autism.	None reported.	Adopted; not known	Mother reported that father had: "mood swings"; Maternal male cousin had behavior problems and delayed speech.	Younger female sibling with autism	Paternal uncle “antisocial” with possible Aspergers; paternal and maternal cousin with”delays”;	None	Brother with speech delay	None	Fraternal twin brother with autism	2nd cousin with autism; grandmother's brother had "some mental illness"
Cause of Death	Drowning	Multiple Injuries	Drowning	Drowning	Drowning	Mestatic Rhabdomysarcoma (Cancer)	Drowning	Drowning	Drowning	Drowning	Drowning
PMI	4	13	33	39	20	22.2	12	16	13	9	13
RIN	7.6	6.9	8.7	7	6.3	7.8	7.4	2.4	6.9	8.5	8.6
Comments	-	Died from accidental fall from 9th story residence..	Significant med history noted child malnourished and neglected prior to adoption; surgery to correct lazy eye in both eyes at age 5; at adoption, low muscle tone & back of skull flattened & ears were dysmorphic (stand up) as a result of being left lying in a crib for extended periods; history of 2 ear infections.	Notes indicated marked obesity, hypogonadism, and high height/weight percentile before age 1; neurologist wanted to check for chromosomal disorder.					Autopsy said child mistakenly given a double dose of med 1 week before death and was treated in the hospital; pm toxicology revealed high level in blood at time of death but about in the normal therapeutic level, but seizures and cardiac arrhythmia are reported complications of the med		

Case	12	13	14	15	16	17	18	19	20	21	22
Age	2	4	5	5	7	8	8	8	9	14	15
Sex	M	F	F	M	M	M	M	M	M	M	F
Diagnosis	Autism	Autism	Autism	Autism	Autism	Autism	Autism	Autism	Autism	Autism	Autism
Basis of Diagnosis	ADI-R	ADI-R	ADI-R	ADOS	ADI-R	ADI-R	Medical Records	ADI-R	ADI-R	ADI-R	ADI-R
ADI Social Score	14	26	24	No ADI	22	19	No ADI	24	24	22	22
ADI Comm Score	9 (NV)	13 (NV)	20 (V)	No ADI	18 (V)	14 (NV)	No ADI	10 (NV)	20 (V)	14 (NV)	21 (V)
ADI R & R Score	6	3	7	No ADI	8	4	No ADI	10	6	8	5
Intellectual Disability	N	Y	Y	Y	Y	N	Y	Y	N	Y	N
Verbal Comprehension	Some words and commands	Fewer than 50 words	Many words (more than 50) and some commands	Some words and commands	Many words (more than 50) and some commands	Most words and language	No ADI- neurologist report states child is able to follow a few commands	Many words (more than 50) and some commands	-	-	Many words (more than 50) and some commands
Verbal Expression	Fewer than 5 words total/ speech not used daily	<Fewer than5 words total / speech not used daily	Functional use of spontaneous language involving three or more word phrases	Fewer than 5 wds total / speech not used daily	Functional use of language with three or more word phrases restricted in frequency and contexts used; echolalia	Functional use of language involving three or more word phrases; occasional echolalia	No ADI – neurologist report states child is non-verbal	Fewer than 5 wds total / speech not used daily	Functional use of language involving three or more word phrases	Fewer than 5 words total / speech not used daily	Functional use of language involving three or more word phrases
Age of 1st Concern	15m	<1yr	2yrs	<24m	2 yrs	36m	No ADI	18m	30m	12m	24m
Language Regression	N	N	N	Y	reported loss of 4 words acquired at age 2 (insufficient language to code true regression on ADI)	N	None Reported	N	N	Y	N
IQ	at 27 months got IQ of 78 on Merrill-Palmer	<50 overall on Bayley Scales	65 on WPPSI	16m age equiv. @ 33m	<50 overall on Bayley Scales	No scores available	No scores available	No scores available	No scores available		
Self injury	N	N	Y	Y	N	N	None reported	N	N	Y	Y
Engagement in Appropriate Activity	Limited constructive play with repetitive activities	Limited constructive play with repetitive activity and motor stereotypies	Engages in passive activities such as watching videos	Limited constructive play with repetitive activity and motor stereotypies	Limited constructive play with repetitive activities	Initiates a limited range of appropriate activities	No ADI- neurologist reports states overactivity and spinning of objects	Engages in passive, but otherwise appropriate activity	Initiates a limited range of appropriate activities, some repetitive	Engages in repetitive play.	Initiates a limited range of appropriate activities, repetitive play
Simplex/ Multiplex	Multiplex	Simplex	Adopted at 10m of age; not known	Simplex	Multiplex	Simplex	Simplex	Simplex	Simplex	Multiplex	Simplex
Seizures	N	N	N	N	N	teacher thought he was having petite mals -- EEG showed "unusual brain activity but not seizures"	Neuro report states dysmorphic features, large head, history of mental retardation	N	N	Y	Y

3. Supplemental Figures

3.1 Figure S1 – Study I Layer-specific expression in DL-PFC

Primary ISH data for laminar markers *CXCL14*, *CALB1*, *RORB*, *PCP4*, *VAT1L*, *NTNG2*, *PDE1A*, and *CTGF* of serial sections from DL-PFC of male autistic and control cases are shown. Boxes outline regions with decreased numbers of ISH-labeled cells.

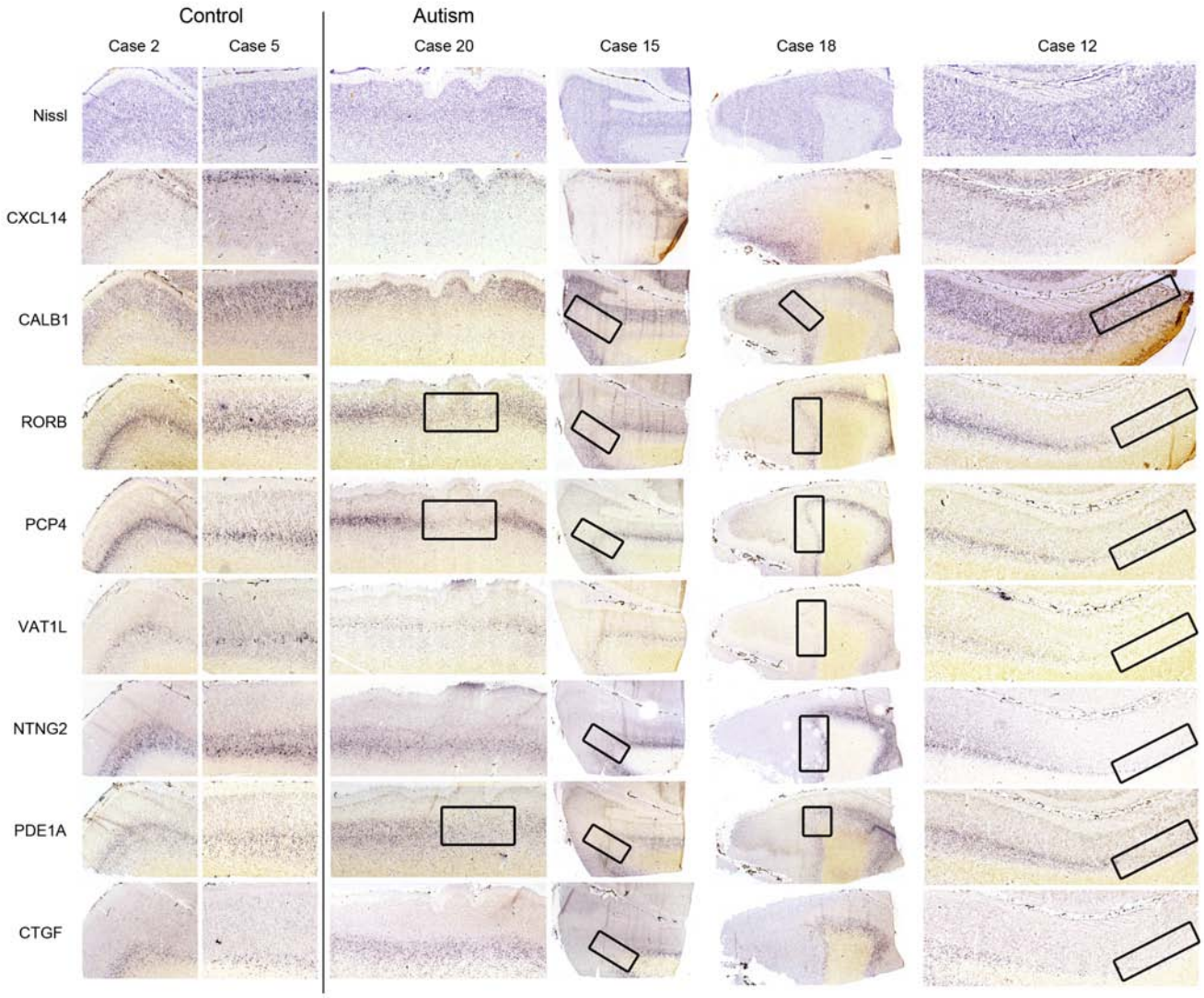

3.2 Figure S2 – Study II Layer-specific expression in DL-PFC

Nissl-stained sections (lines demarcate lamina) and ISH images of *NEFL*, *CALB1*, *RORB*, and *PCP4* in 4 female cases 1, 6, 13, and 22 are shown. Images for *NEFL*, *CALB1*, *RORB*, and *PCP4* were contrast-adjusted equally for visibility across cases. Aberrant expression of three or more of shown genes was evident in autistic and control cases. Decreased expression of ISH labeling was also observed in female control case 6. Boxes outline regions with decreased ISH labeling. Scale bars: 1 mm.

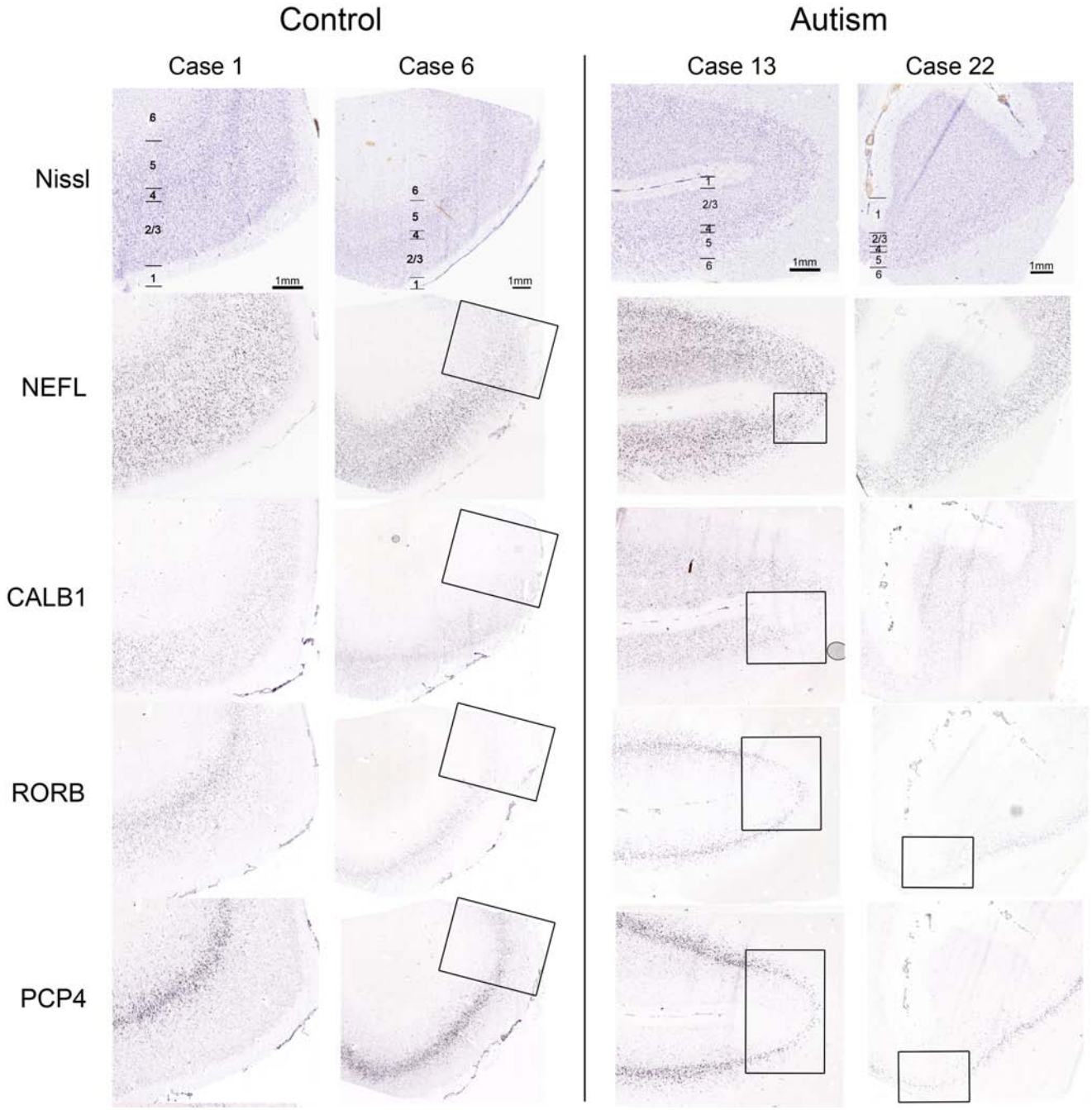

3.3 Figure S3 – Study II Layer-specific expression in PSTC

Nissl-stained sections (lines demarcate lamina) and ISH images for *NEFL*, *CALB1*, *RORB*, and *PCP4* markers are shown in pSTC of male autistic and control cases. ISH images were contrast-adjusted equally for visibility across cases. Boxes outline areas with decreased numbers of ISH-labeled cells in autistic cases. Scale bars: 1mm.

<image on next page>

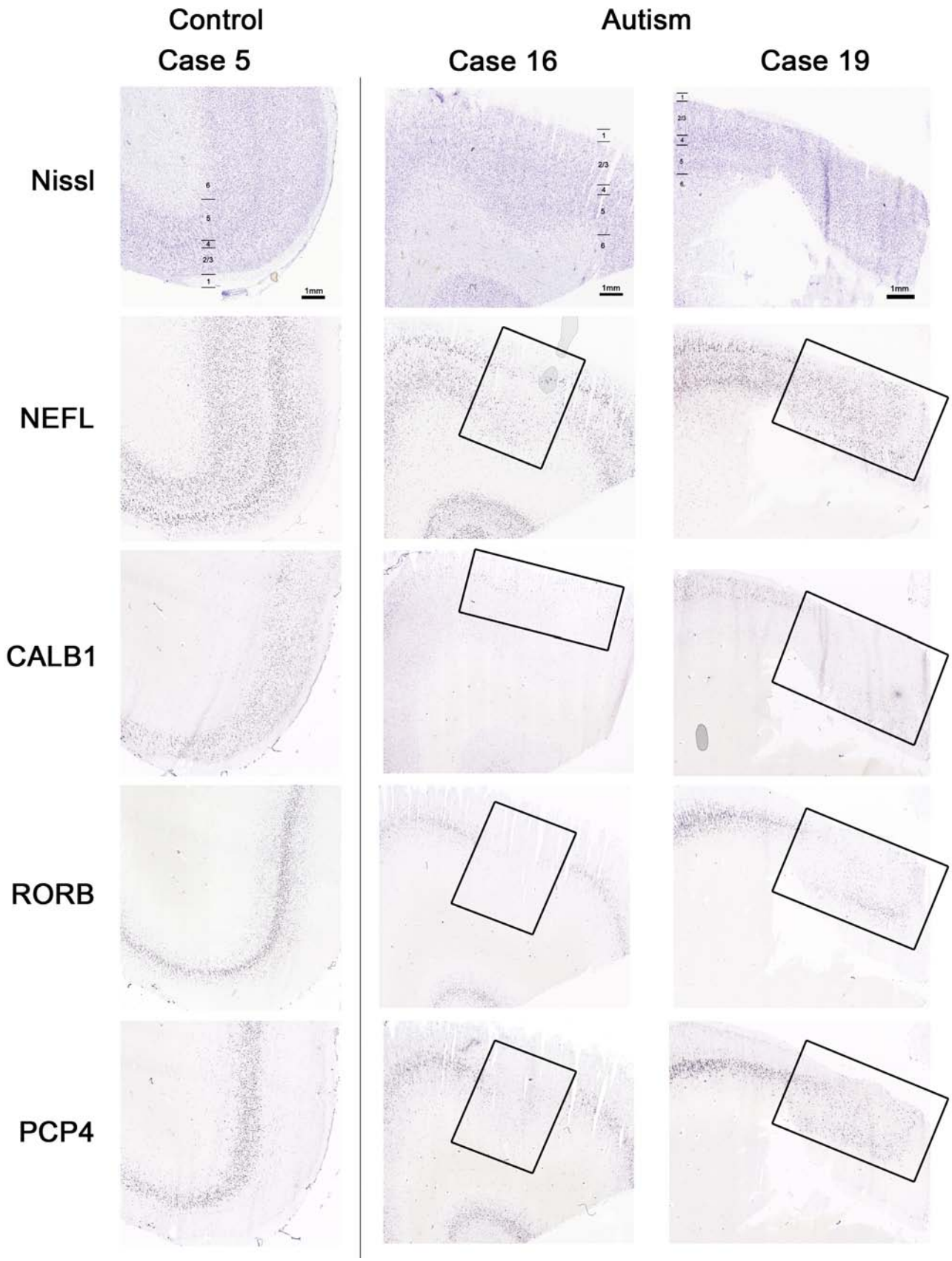
Control
Autism
Case 5
Case 16
Case 19
Nissl
NEFL
CALB1
RORB
PCP4
1mm

3.4 Figure S4 – Study II Layer-specific expression in OCC

Nissl-stained sections (lines demarcate lamina) and ISH images for *NEFL*, *RORB*, *PCP4* and *PDE1A* markers are shown in occipital cortex of male autistic and control cases. ISH images were contrast-adjusted equally for visibility across cases. No areas of aberrant expression were evident in ISH images of autistic and control cases in these samples. Scale bars: 1mm.

<image on next page>

Appendix: *Patches of Disorganization in the Neocortex of Children with Autism*

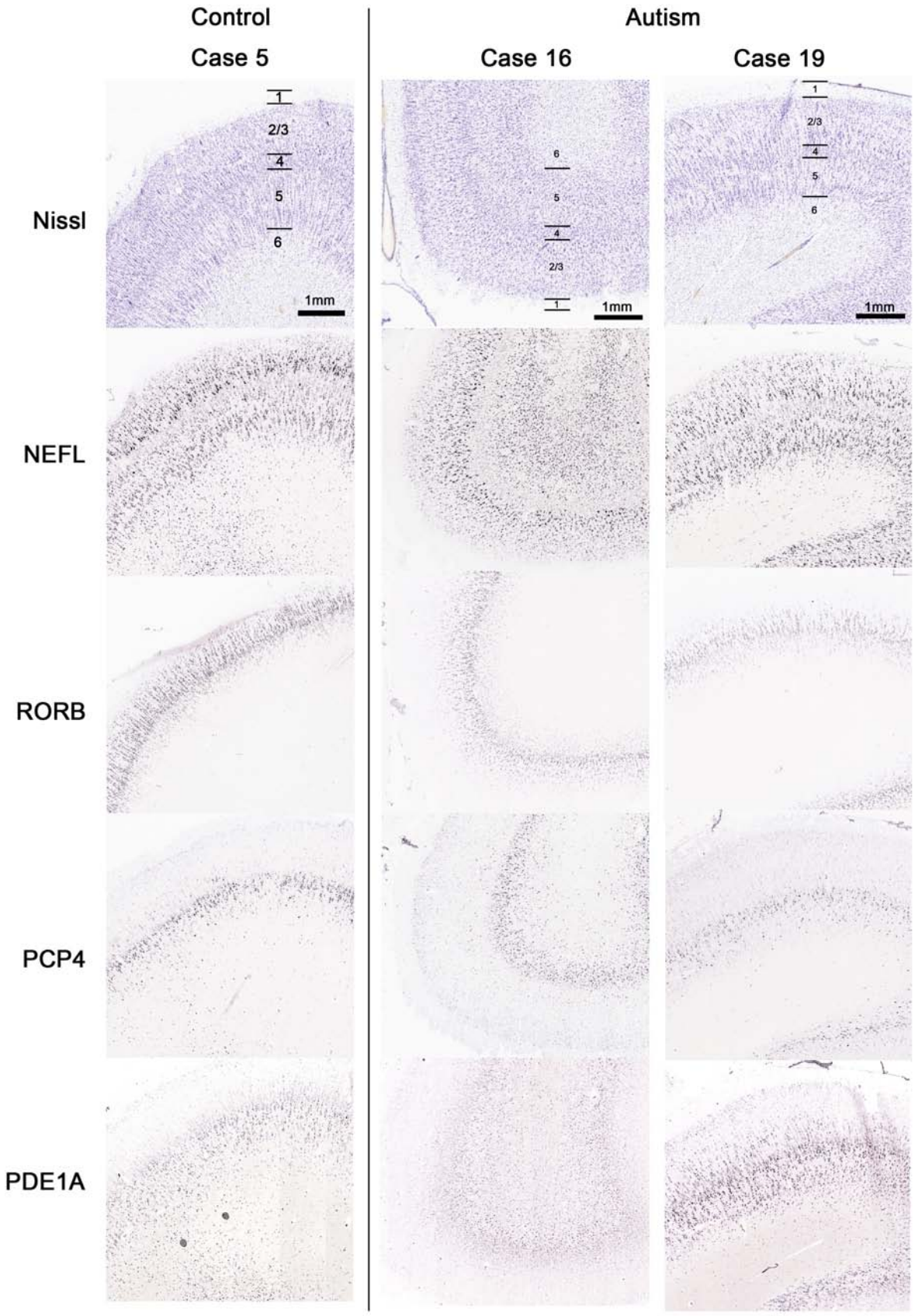

3.5 Figure S5 – Autism patch region overlays

Image overlays for autism cases 12 and 15 showing focal regions of aberrant expression adjacent to "normally-appearing" cortex.

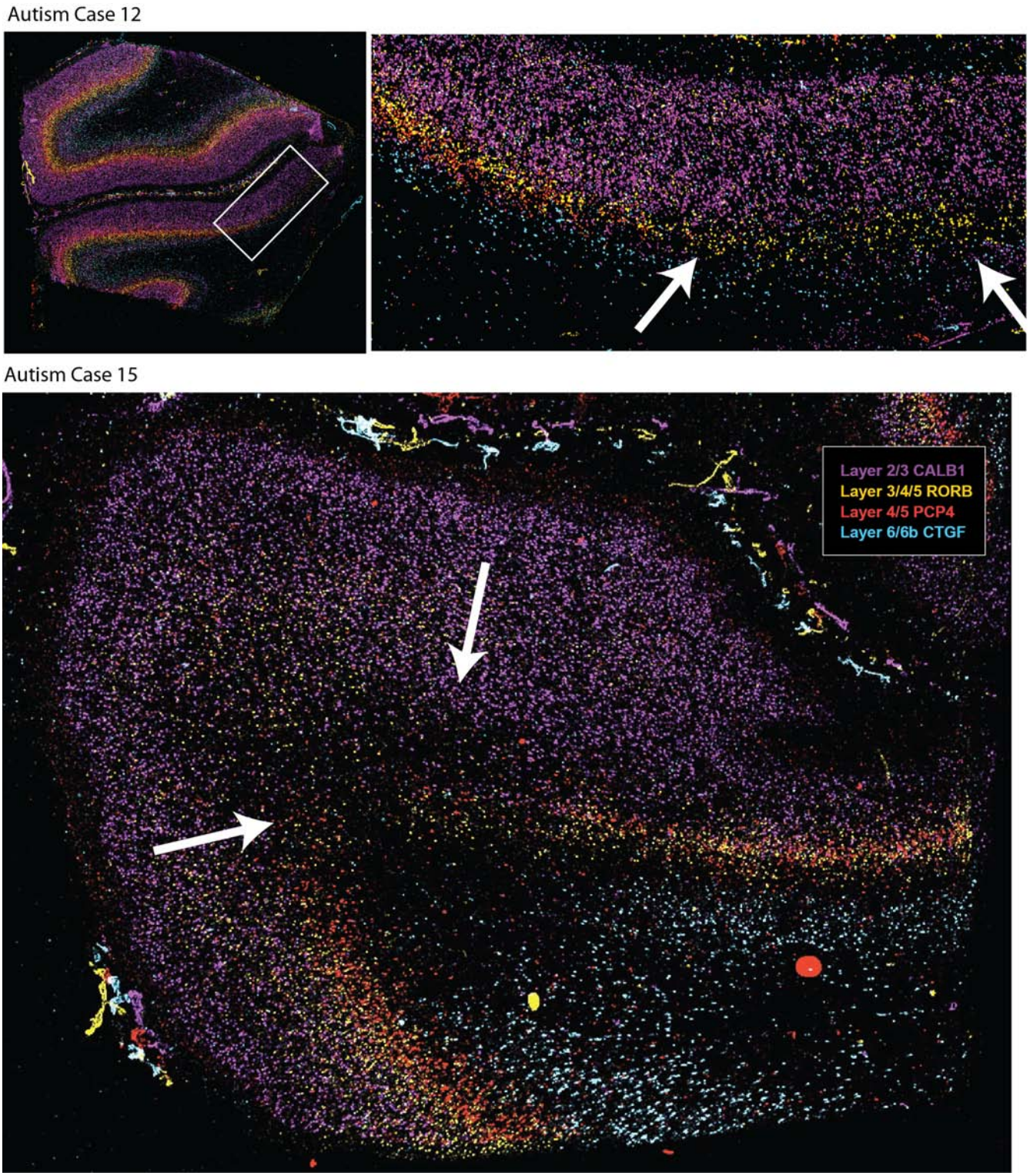

3.6 Figure S6 – Reconstruction workflow

The reconstruction workflow was comprised of three steps: stack registration, point cloud extraction, and volume generation. The first two steps operated in parallel to produce a set of 2D transformations for a rigid body registration and a list of point cloud data for each processed image. The two intermediates then were combined in the third step to produce registered volume stacks that can be loaded directly into UCSF Chimera visualization software. For more details, see S1.3.2.

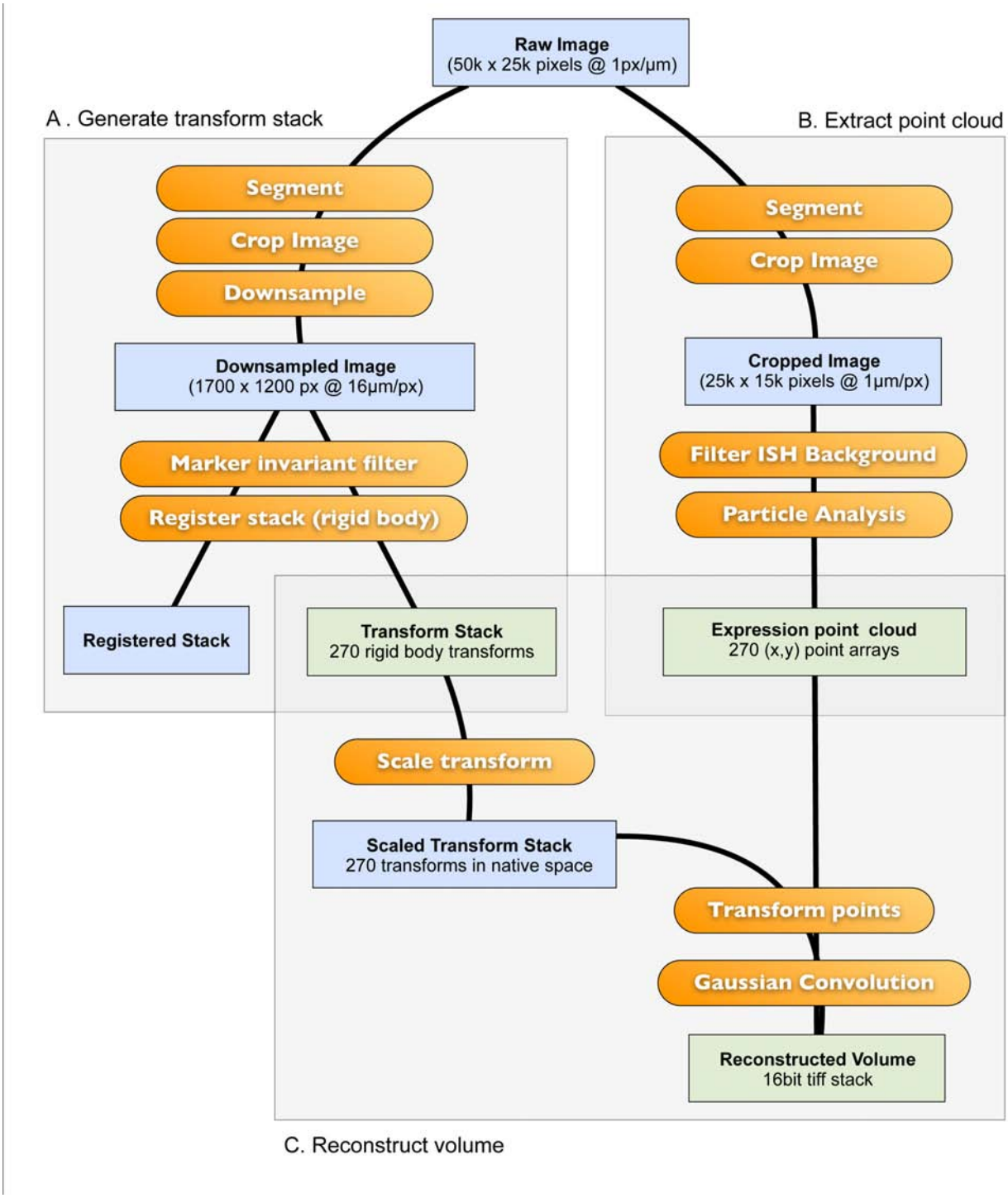

3.7 Figure S7 – Control reconstruction, step-wise

Reconstruction of control case 4 from four layer-specific markers is shown. The three-step diagram shows the reconstruction process. First, layers of pseudo-expression density clouds were generated from extract point cloud information. Second, images were recombined into a single stack. Finally, the image stacks were interpolated to generate the final volume stack.

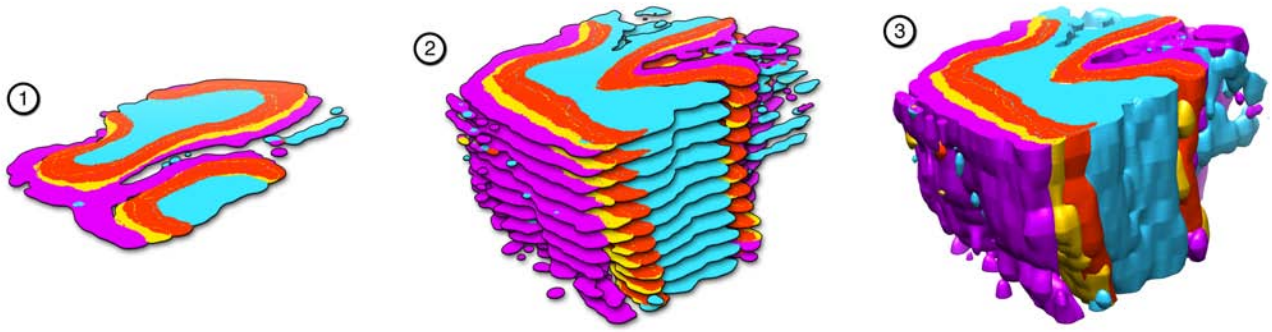

3.8 Figure S8 – Stereological estimates of neuron and glia density

Top panel: Mean neuron and glia cell volumes, grouped and per region. (Error bars: standard deviation). Bottom panel: Average neuron and glia density, grouped and per region (Error bars: standard deviation). A one-factor ANOVA revealed no significant differences in neuron volume, neuron density, glia volume, or glia density between groups across the independent stereological regions (N=8 per region, N=8, p=0.059). When grouped by diagnostic category, a small but significant increase in neuron density in the autism cortex (two-tailed T, p=0.031, N=16 per group) relative to control cortex was identified.

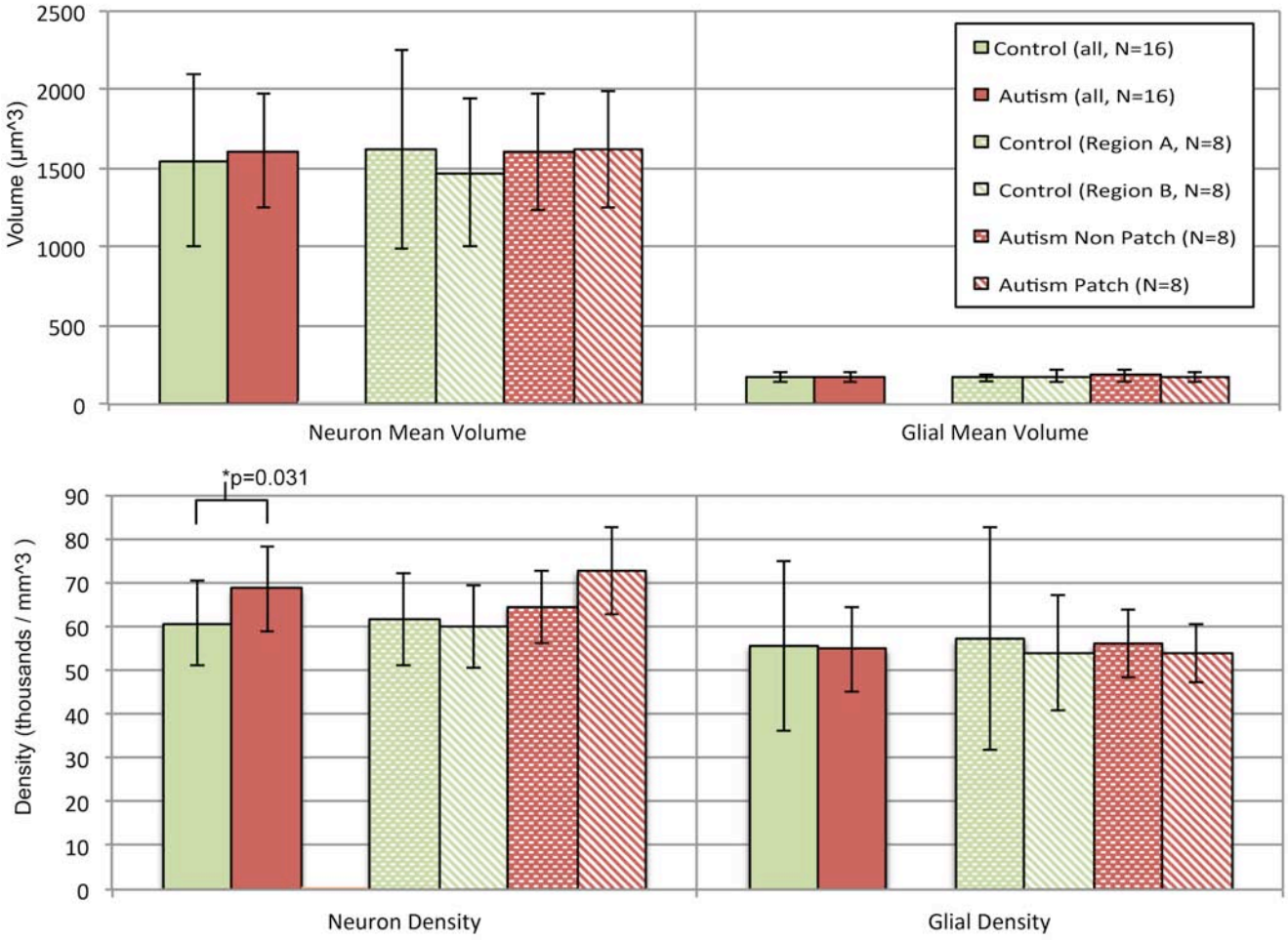

3.9 Figure S9 – ISH images of glial markers

Primary ISH images of glial markers GAD1 and SLC1A2, along with nearest Nissl-stained section, taken from DL-PFC of male autistic and control cases. The arrowhead indicates the singular region of abnormal glial marker labeling found in autistic tissue (Case 12). Scale bars: 1mm.

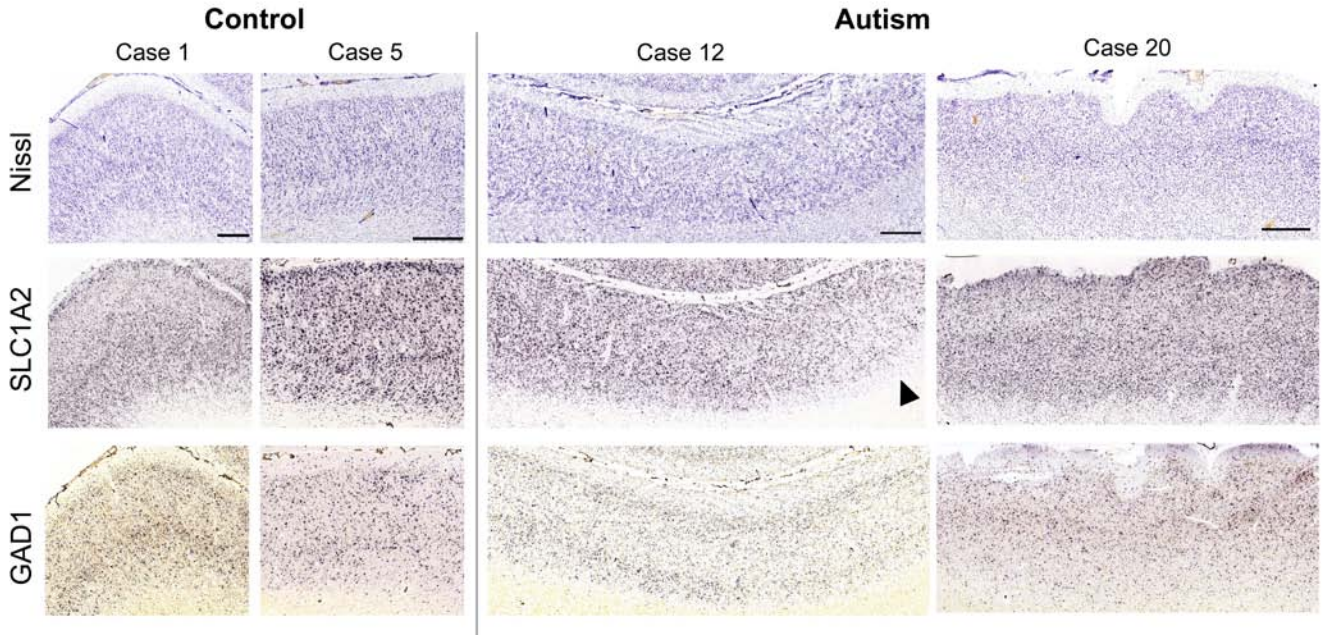

4. Supplemental References

1. Lord C, Rutter M, Le Couteur A. Autism Diagnostic Interview-Revised: a revised version of a diagnostic interview for caregivers of individuals with possible pervasive developmental disorders. J Autism Dev Disord 1994;24(5):659–685.

2. Lord C, Risi S, Lambrecht L, et al. The autism diagnostic observation schedule-generic: a standard measure of social and communication deficits associated with the spectrum of autism. J Autism Dev Disord 2000;30(3):205–223.

3. Rehen SK, Yung YC, McCreight MP, et al. Constitutional aneuploidy in the normal human brain. J Neurosci 2005;25(9):2176–2180.

4. Lein ES, Hawrylycz MJ, Ao N, et al. Genome-wide atlas of gene expression in the adult mouse brain. Nature 2007;445(7124):168–176.

5. Braak, E. On the structure of lamina IHab pyramidal cells in the human isocortex. A Golgi and electron-microscopical study with special emphasis on the proximal axonal segment. J Hirnforsch 1980;21:439-444.

6. Kandel, Eric R., James H. Schwartz, and Thomas M. Jessell, eds. Principles of neural science. Vol. 4. New York: McGraw-Hill, 2000.

7. Gundersen HJ, Jensen EB, Kiêu K, Nielsen J. The efficiency of systematic sampling in stereology--reconsidered. Journal of Microscopy 1999;193(Pt 3):199–211.

8. Mouton PR. Principles and Practices of Unbiased Stereology: An introduction for Bioscientists. Johns Hopkins University Press, 2002.

9. West MJ, Gundersen HJ. Unbiased stereological estimation of the number of neurons in the human hippocampus. J Comp Neurol 1990;296(1):1–22.

10. West MJ, Slomianka L, Gundersen HJ. Unbiased stereological estimation of the total number of neurons in thesubdivisions of the rat hippocampus using the optical fractionator. Anat Rec 1991;231(4):482–497.

11. Jensen, E.B.V. & Gundersen, H.J.G. The rotator. *Journal of Microscopy* **170**, 35-44 (1993).

12. Mouton PR, Pakkenberg B, Gundersen HJ, Price DL. Absolute number and size of pigmented locus coeruleus neurons in young and aged individuals. J Chem Neuroanat 1994;7(3):185–190.